PNAS
www.pnas.org

Supplementary Information for

Otogelin, otogelin-like, and stereocilin form links connecting outer hair cell stereocilia to each other and the tectorial membrane

Paul Avan, Sébastien Le Gal, Vincent Michel, Typhaine Dupont, Jean-Pierre Hardelin, Christine Petit[1], and Elisabeth Verpy[1]

[1]C.P. and E.V. contributed equally to this work

Correspondence : Christine Petit or Elisabeth Verpy
Email: christine.petit@pasteur.fr or elisabeth.verpy@pasteur.fr

This PDF file includes:

www.pnas.org/cgi/doi/10.1073/pnas.1902781116

Supplementary materials and methods

Animals

The *Otogl* conditional knockout mouse lines were established at the MCI/ICS (Mouse Clinical Institute - *Institut Clinique de la Souris* -, Illkirch, France; http://www-mci.u-strasbg.fr). The targeting vector was constructed as follows. A 2.3 kb fragment encompassing *Otogl* exons 5 and 6 was amplified by PCR (from RP23-193K15 BAC genomic DNA) and inserted into a proprietary MCI vector. This MCI vector contains a LoxP site and a floxed and flipped neomycin resistance cassette. A 4.4 kb fragment corresponding to the 5' homology arm and a 2.9 kb fragment corresponding to the 3' homology arm were amplified by PCR, and inserted into a step1 plasmid to generate the final targeting construct. The linearized construct was introduced into C57BL/6N mouse embryonic stem (ES) cells by electroporation. The target clones were selected on G418, and identified by long-range PCR with external primers, with confirmation by Southern blot analysis with an internal *neo* probe and a 3' external probe. Two correct recombinant ES clones were injected into BALB/cN blastocysts. The resulting male chimeras were crossed with FlpO deleter mice (1) to obtain germline transmission of the recombinant *Otogl* allele. Efficient Flp-mediated excision of the flipped *neo* cassette was achieved with the maternal contribution, and heterozygous conditional knockout mice were obtained. These mice were crossed with PGK-*cre*^{m} transgenic mice carrying the cre recombinase gene driven by the early-acting, ubiquitous phosphoglycerate kinase 1 gene promoter (2), leading to otogelin-like-null mice (*Otogl*$^{tm1Ugds/tm1Ugds}$) with a frameshift deletion of *Otogl* exons 5 and 6. Routine genotyping of the mutant mice was performed by two PCR amplifications with the oligonucleotide Ef-7596 (5′-GGAGCCTCAGTACACAGTATGGG-3′) overlapping the exon 6-intron 6 boundary or Lf-7592 (5'-GTGCAGGGAATCATGTACAGCTTGG-3'), binding within intron 4, as the forward primer, and oligonucleotide Er-7597 (5'-GTAAACACATGATATTTCTCCACAGCC-3'), binding within intron 6, as the reverse primer. The absence of otogelin-like in these mice was confirmed by immunofluorescence experiments on whole-mount preparations of the organ of Corti. All studies were performed on mixed genetic backgrounds.

We have previously reported the production of *Strc*$^{tm1Ugds/tm1Ugds}$ (3), *Otog*$^{tm1Prs/tm1Prs}$ (4), *Ush1c*$^{tm1.1Ugds/tm.1.1Ugds}$ (5), *Cdh23*$^{tm1.2Ugds/tm1.2Ugds}$ (6), *Pcdh15*$^{\Delta ex5/\Delta ex5}$ (7), *Ush1g*$^{tm1.2Ugds/tm1.2Ugds}$ (8) and *Pcdh15*$^{\Delta'CD2/\Delta'CD2}$ (7) mice, with defects of stereocilin, otogelin, harmonin, cadherin 23, protocadherin 15, SANS, and the CD2 isoforms of protocadherin 15, respectively. *Tecta*$^{\Delta ENT/\Delta ENT}$ mice (9) and *Myo7a*$^{4626SB/4626SB}$ mice (10) were kindly provided by Dr Guy Richardson (University of Sussex, Falmer, UK) and Dr Karen P. Steel (Sanger Institute, Cambridge, UK), respectively. *Strc*$^{tm1Ugds/tm1Ugds}$,*Tecta*$^{\Delta ENT/\Delta ENT}$ double-knockout mice were produced by crossing *Strc*$^{tm1Ugds/tm1Ugds}$ and *Tecta*$^{\Delta ENT/\Delta ENT}$ mice, and then intercrossing the double heterozygous offspring. Likewise, *Pcdh15*$^{\Delta ex5/\Delta ex5}$,*Cdh23*$^{tm1.2Ugds/tm1.2Ugds}$ double-knockout mice were produced by crossing *Pcdh15*$^{+/\Delta ex5}$ mice with *Cdh23*$^{+/tm1.2Ugds}$ mice, and then intercrossing the double heterozygous offspring. However, in this second case, double-knockout mice were very rarely obtained because of the genetic linkage between the two genes (located 13 Mb apart on mouse chromosome 10).

Recordings of auditory brainstem responses (ABR), cochlear microphonics (CM), compound action potentials (CAP), and distortion-product otoacoustic emissions (DPOAE).

Mice were anesthetized (150 mg/kg ketamine, 2 mg/kg levomepromazine, with additional half doses every 30 minutes), and placed on a temperature-controlled blanket (set to maintain core temperature at 37°C) in a sound-proof booth. For ABR recordings, subcutaneous steel electrodes (active: ipsilateral mastoid; passive: vertex; ground: neck muscles) connected to a Grass P511 preamplifier (gain x 100 000) collected the electrical potentials from the auditory pathways in response to tone bursts at frequencies between 5 and 40 kHz, with stepwise increases in intensity from 0 to 115 dB SPL. The ABR threshold was defined as the lowest tone-burst level, with a resolution of 5 dB, at which, after the averaging of 250 epochs, the ABR trace displayed at least one repeatable wave. For CM and CAP recordings, the active electrode was surgically placed in the round-window niche. After x 10 000 amplification with the ABR preamplifier, we collected signals corresponding to the receptor potentials of basal sensory cells (from which the CM is generated) and the synchronous activity of the cochlear nerve fibers (leading to the CAP)

in response to tone bursts, and analyzed CM waveforms relative to the sound stimulus. The baseline value of the CM before the onset of the stimulus is 0 μV, and the CM switches on after 0.3 ms (corresponding to the time for sound propagation from the earphone to the cochlear windows), and the compound action potential then follows. Beyond 2 ms after the stimulus, the round-window response corresponds to the CM only. For CAP masking tuning curves, the sound stimuli used were mixtures of one tone-burst at 10 kHz, 10 dB above CAP threshold, and an interfering continuous masker tone of varying frequency. For the superimposed continuous sound to mask the responses of the probe-sensitive neurons, resulting in a decrease in CAP amplitude, the intensity of the masking tone must be high enough to stimulate the probe-sensitive neurons and swamp their responses to the probe despite the difference between probe and masker frequencies. At each masker frequency, the masker level was roved until the amplitude of the CAP in response to the test tone-burst was halved. For both ABR and CAP, the tone-burst stimuli were produced by a Wavetek-70 arbitrary waveform generator (2-period rise and decay times, 16-period plateau), and sent to a Radio Shack tweeter (40-1376, 8 Ω – 70 W) connected to a conical tip designed to fit optimally into the mouse external ear canal. This setup was calibrated *in situ* with a probe microphone (PCB-Larson-Davis ¼ inch 2520; preamplifier PCB 480C02) connected to a frequency analyzer (Adobe Audition v.1.5). For DPOAE, a miniature microphone probe sealed in the external ear canal was used to record responses to two-tone stimuli (equal level primary tones f_1 and f_2, with $f_2/f_1 = 1.20$, and f_2 swept in $1/10^{th}$ octave steps from 4 to 31 kHz) and the combination tone at $2f_1$-f_2 was extracted. Stimulus levels were varied stepwise from 20 to 75 dB SPL.

Antibodies

The rabbit polyclonal anti-stereocilin antibody directed against the synthetic peptide CFLSPEELQSLVPLSD (amino acids 970-985, RefSeq accession number NP_536707.2) has been described elsewhere (3, 11). The rabbit polyclonal anti-otogelin and anti-otogelin-like antibodies were directed against two synthetic peptides of the murine otogelin (SELHPDPELSRERTC, amino acids 881-895 and CDPGLCEAEQVPTCREDQ, amino acids 2528-2545, RefSeq accession number NP_038652.2) and otogelin-like (CTDREEHPRSAGEIWN, amino acids 1838-1853 and CLNDAPYKQKRSGFFLE,

amino acids 1005-1020, RefSeq accession number NP_001171038.1) amino acid sequences, respectively. All antibodies were affinity-purified on the corresponding peptides. The specificity of each antibody was confirmed by demonstrating that immunoreactivity was lost in the cochlea of mutant mice lacking the corresponding protein.

Immunostaining of whole-mount organs of Corti

Inner ears were fixed by incubation in 4% paraformaldehyde in phosphate-buffered saline (PBS) pH 7.4 for one hour at room temperature before microdissection. The tissues were washed three times in PBS, and then incubated in PBS containing 1% bovine serum albumin for one hour at room temperature, before overnight incubation at 4°C with the primary antibodies. For the detection of immunofluorescence signals, the samples were washed three times in PBS, and then incubated at room temperature for one hour with Atto-488-conjugated goat anti-rabbit IgG fragment (1/500, Sigma-Aldrich) and Atto-565-conjugated phalloidin (0.5 µM, Sigma-Aldrich) to stain actin. The samples were then washed three times in PBS, and subjected to terminal fine microdissection of the sensory epithelium (organ of Corti) for mounting in FluorSave™ Reagent (Calbiochem) and imaging with a LSM700 Meta confocal microscope (Carl Zeiss) equipped with an oil-immersion Plan-Apochromat 63X/1.4 NA objective lens (Carl Zeiss). The first steps in immunolabeling before scanning electron microscopy were the same as those for immunofluorescence detection, except that primary antibodies were detected with protein-A-conjugated 15 nm colloidal gold particles (EM Laboratory, Utrecht University, The Netherlands; diluted 1:50 in PBS containing 1% bovine serum albumin). Finally, samples were post-fixed by incubation for one hour in 2.5% glutaraldehyde in 0.1 M sodium cacodylate buffer for scanning electron microscopy.

Scanning electron microscopy

Inner ears were fixed by overnight incubation at 4°C in 2.5% glutaraldehyde in 0.1 M sodium cacodylate buffer. After five brief washes in sodium cacodylate buffer, the organ of Corti was microdissected, and processed according to the osmium tetroxide/thiocarbohydrazide (OTOTO) impregnation method, as previously described (12). The samples were then dehydrated in graded ethanol solutions and subjected to

critical point drying with liquid CO_2, before mounting on aluminum stubs with carbon tab adhesive (Agar Scientific, Essex, UK). Specimens were imaged in a JEOL JSM-6700 F scanning electron microscope (JEOL, Tokyo, Japan) operating at 3-5 kV. When immunolabeling was coupled to scanning electron microscopy, dried specimens were mounted with colloidal silver adhesive (Agar silver paint, Agar Scientific) to enhance their conductivity. Samples were then coated with 20-30 nm of carbon, and imaged with an Yttrium Aluminum Garnet (YAG) back-scatter detector.

Localization of stereocilin in transfected cells

Two overlapping fragments covering the full-length mouse *Strc* cDNA were obtained from the vestibular end organs of newborn mice by RT-PCR with the primers 5'-CAGAAGCTTCATGGTGAGCATAGCCAGAACTC-3' (*Hin*dIII restriction site underlined) and 5'-CACCTGCTGCACCCATATTTTTAAC-3' for the 5' fragment and primers 5'-GCATGCTGGGCCCCTTGTT-3' and 5'-CTGGTCGACTTAATAGGTGGCCAAAAATGCTGAC-3' (*Sal*I restriction site underlined) for the 3' fragment. The two PCR fragments were inserted into the Topo® TA vector (Thermo Fisher Scientific) for the selection of clones without mutations. Inserts were excised with *Hind*III and *Sca*I (restriction site located in the region of overlap) for the 5' fragment, and *Sca*I and *Sal*I for the 3' fragment. The two inserts were then joined and inserted into the pEGFP-N1 (Clonetech) expression vector to produce a stereocilin-EGFP fusion protein containing a C-terminal EGFP tag. The fusion protein was retained intracellularly, and was not recognized by anti-EGFP antibodies. We therefore excised a *Bam*HI-*Not*I fragment encoding the C-terminal part of stereocilin fused to EGFP from the recombinant expression vector (pStrc-EGFP), and replaced it with a fragment containing only the 3' end of the *Strc* cDNA. This fragment was obtained by PCR amplification from pStrc-EGFP, with the forward primer 5'-CATGACCTGCGAGTTTCTG-3' and the reverse primer 5'-TTGCGGCCG**CTA**TAATAGGTGGCCAAAAATGCTGAC-3' (*Not*I restriction site underlined and *Strc* stop codon in bold), insertion into Topo® TA, and digestion with *Bam*HI and *Not*I. This recombinant expression vector was used to transfect HeLa cells or MDCK cells in the presence of Lipofectamine™ 2000 (Invitrogen). Immunocytofluorescence experiments were performed as described above for whole-

mount organs of Corti, after the cells had been fixed by incubation in 4% paraformaldehyde for 15 minutes, washed twice in PBS, and incubated in 50 mM NH_4Cl in PBS for 15 minutes, and then washed three times in PBS. TRITC-conjugated wheatgerm agglutinin (10 μg/ml, Sigma-Aldrich) was used to stain the cell-surface glycoproteins.

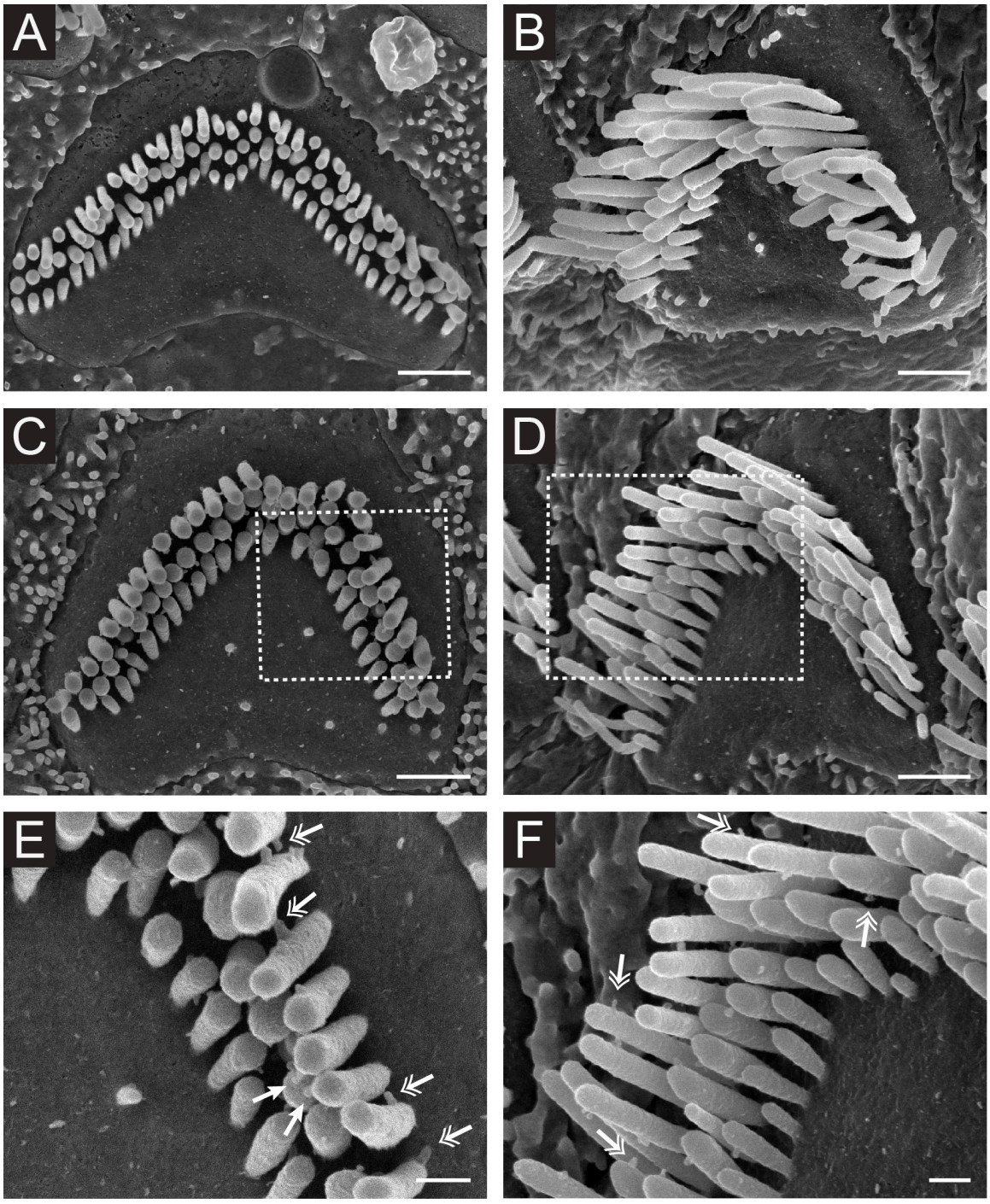

Fig. S1. OHC hair bundles in P14 *Otogl*$^{-/-}$ mice. Protrusions emerging on the lateral sides of OHC stereocilia (double arrows in E and F), or at the position of the tip links (arrows in E), are numerous in some bundles (C-F), but not in others (A, B). E and F are enlargements of the regions boxed in C and D, respectively. Scale bars: 1 μm (A-D), 0.3 μm (E, F).

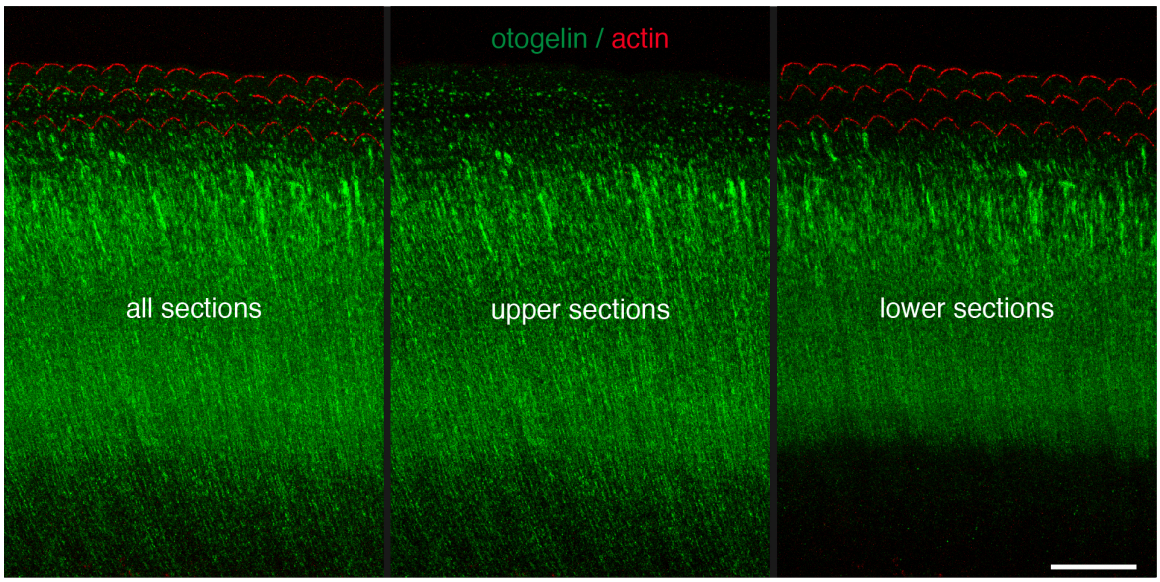

Fig. S2. Localization of otogelin-containing structures of the TM relative to the anchoring points of the OHC tall stereocilia. Left panel: compression of all confocal images of a TM whole-mount preparation immunostained for otogelin (in green), and stained for actin (in red), in P15 mice. Actin staining reveals the tips of stereocilia lifted off and embedded in the TM. Separate compression of the seven upper (middle panel) and twelve lower (right panel) sections shows punctate labeling in the upper part of the TM, in the region above the OHCs, and an absence of otogelin-immunoreactive fibers in the region of the TM in which the tips of the OHC tall stereocilia are embedded. Scale bar: 20 μm.

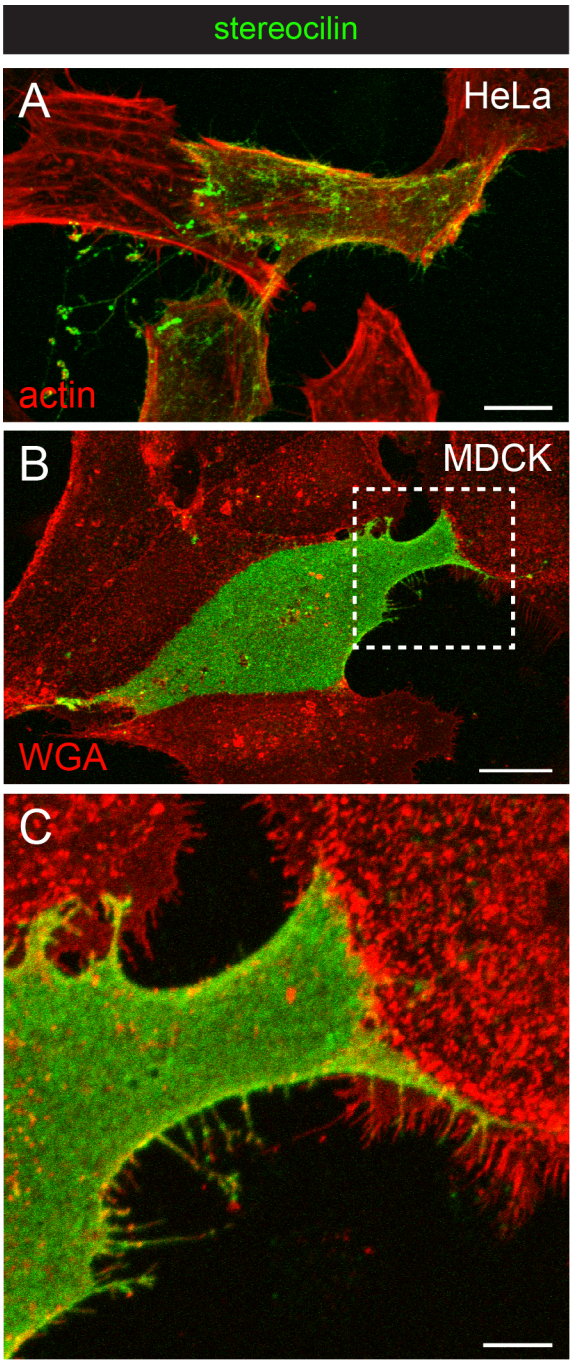

Fig. S3. Stereocilin at the surface of the plasma membrane in transfected cells. Transiently transfected HeLa (A) and MDCK cells (B, C) producing stereocilin. The actin cytoskeleton is stained in red with phalloidin in A, and the outer surface of the plasma membrane is stained in red with wheatgerm agglutinin in B and C. A higher magnification of the area boxed in B is shown in C. Stereocilin immunostaining (green) is observed on the outer surface of transfected cells, but not on the untransfected neighboring cells. Note the abundance of stereocilin at the surface of filopodia in the transfected cells. Scale bars: 10 µm (A), 20 µm (B), or 5 µm (C).

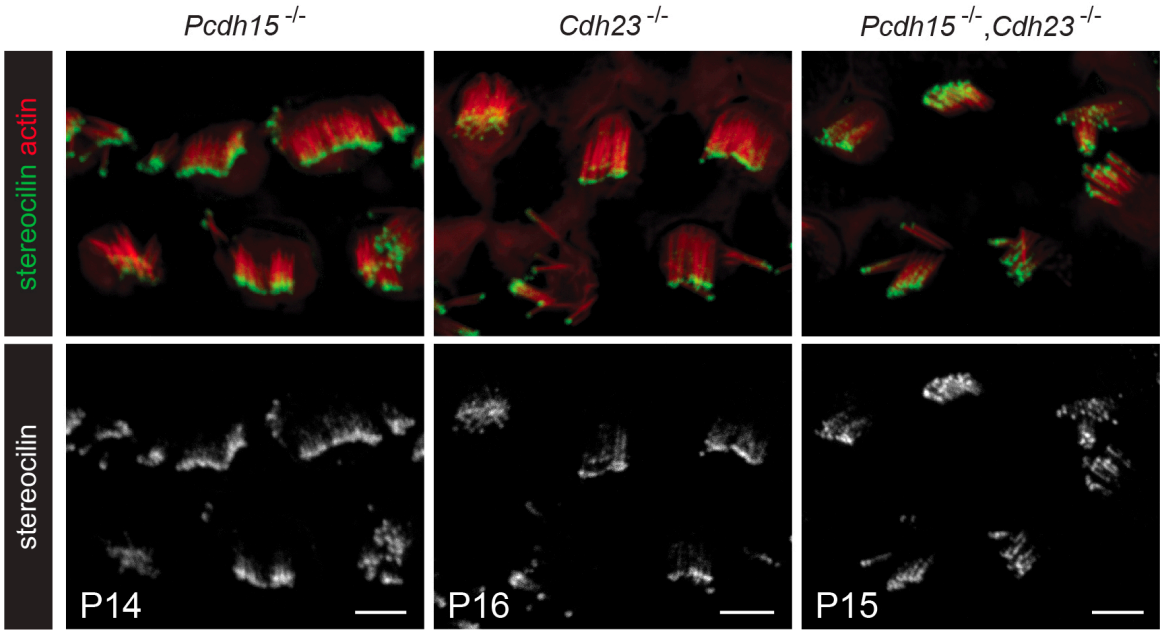

Fig. S4. Localization of stereocilin in the mature OHCs of *Pcdh15*$^{-/-}$ mice, *Cdh23*$^{-/-}$ mice, and *Pcdh15*$^{-/-}$,*Cdh23*$^{-/-}$ double-mutant mice. Confocal images of P14-P16 OHCs immunostained for stereocilin (green or white), and stained for actin (red). *Pcdh15*$^{-/-}$ mice and *Cdh23*$^{-/-}$ mice lack protocadherin 15 and cadherin 23, respectively, and *Pcdh15*$^{-/-}$,*Cdh23*$^{-/-}$ mice lack both cadherin-related proteins. Stereocilin staining is strong at the tips of the stereocilia, and extends abnormally between adjacent stereocilia. Hair bundle fragmentation is no worse in the double-mutant mice than in the single-mutant mice, indicating that, during hair bundle development, stereocilia are also interconnected by transient lateral links containing neither cadherin-related protein. Scale bars: 3 μm.

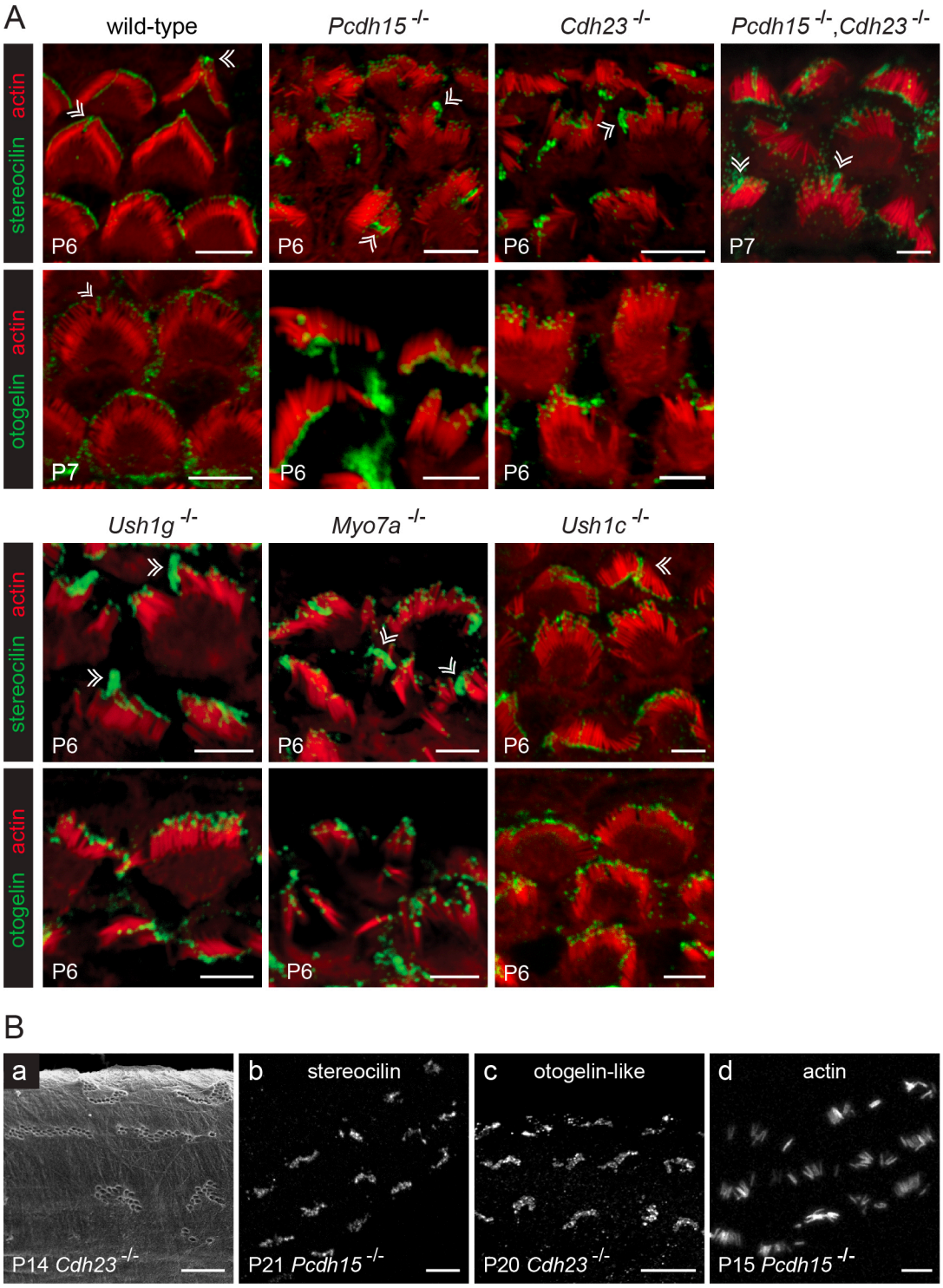

Fig. S5. Interaction of OHC hair bundles with the tectorial membrane in mouse models of Usher syndrome of type 1 (Ush1). (A) Confocal images of P6-P7 OHCs immunostained for either stereocilin or otogelin (green), and stained for actin (red). The genotypes of the mutant mice are indicated: *Pcdh15*$^{-/-}$ mice and *Cdh23*$^{-/-}$ mice lack protocadherin 15 and cadherin 23, respectively, and *Pcdh15*$^{-/-}$,*Cdh23*$^{-/-}$ mice lack both

cadherin-related proteins. *Ush1g*$^{-/-}$ mice, *Myo7a*$^{-/-}$ mice, and *Ush1c*$^{-/-}$ mice lack SANS, myosin VIIa, and harmonin, respectively. Stereocilin and otogelin are detected only at the tips of the tall stereocilia in wild-type mice, whereas both proteins are detected at the tips of all stereocilia in Ush1 mouse models. Double arrowheads indicate the transient kinocilium still present in some hair cells at this stage. (B) Scanning electron micrograph (a) and confocal images (b-d) of the tectorial membrane in P14-P21 mice. In *Cdh23*$^{-/-}$ mice and *Pcdh15*$^{-/-}$ mice, scanning electron microscopy (a) and stereocilin (b) or otogelin-like (c) immunostainings of the lower surface of the TM indicate that, for each OHC, stereocilia from several rows are connected with the TM. Actin staining in a *Pcdh15*$^{-/-}$ mouse (d) reveals clumps of stereocilia, torn off from the apical surface of OHCs and stuck to the TM. Such abnormally torn off clumps of stereocilia were also observed, although to a lesser extent, in the other Ush1 mutants. These results suggest that the fragmented OHC hair bundles observed after TM removal in these mutants may not always reflect the actual condition in vivo. Scale bars: 5 µm (A and panels b-d in B) or 2 µm (panel a in B).

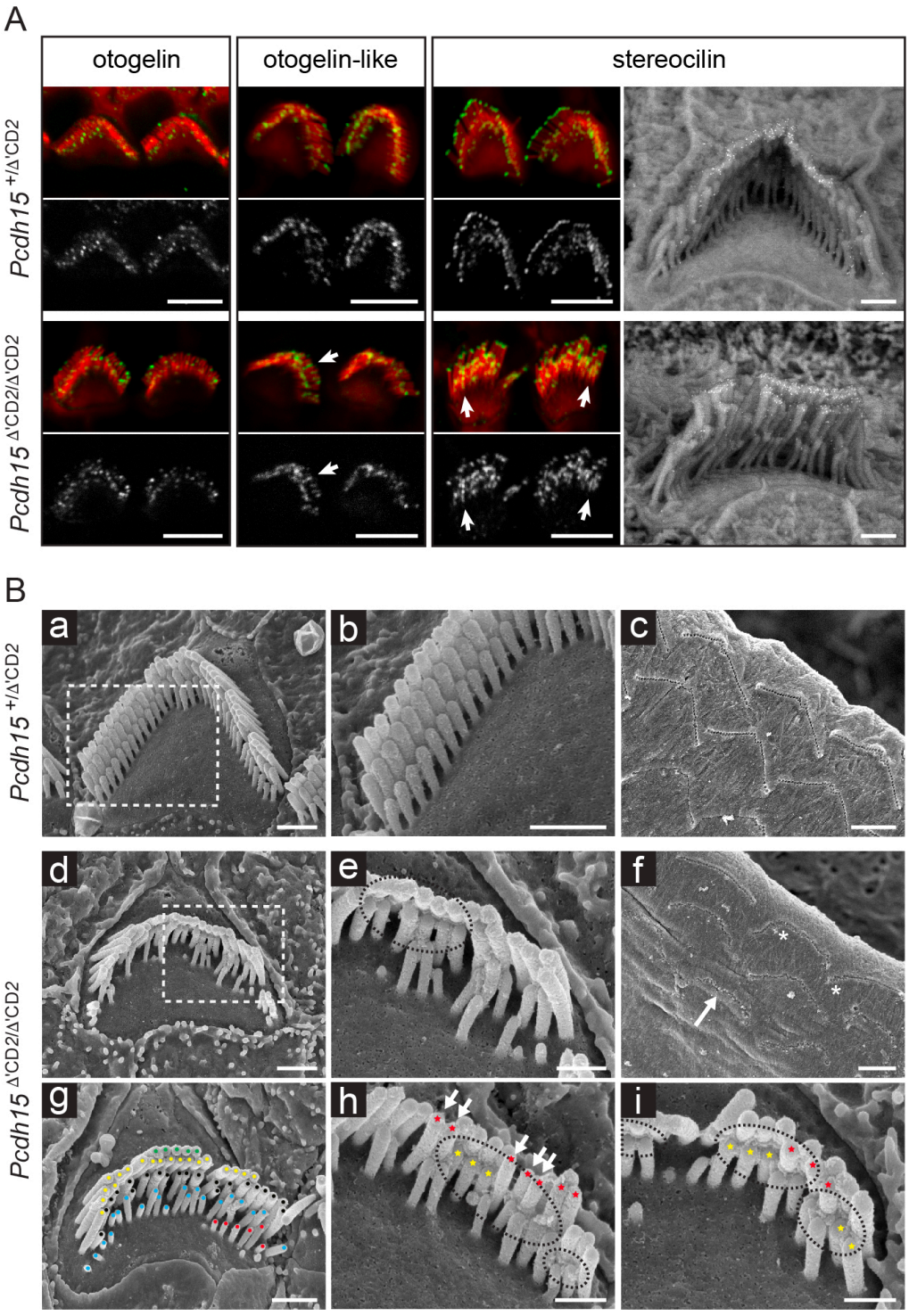

Fig. S6. Localization of otogelin, otogelin-like, and stereocilin, and distribution of lateral links in the OHCs of PCDH15-CD2-deficient mice. (A) Confocal images of OHCs immunostained for otogelin, otogelin-like, or stereocilin (green or white), and stained for actin (red), and scanning electron micrographs of OHC hair bundles after stereocilin immunolabeling, in *Pcdh15*$^{+/\Delta'CD2}$ control mice (upper panels) and

Pcdh15$^{\Delta'CD2/\Delta'CD2}$ mutant mice lacking CD2 isoforms of PCDH15 (lower panels) on P30. In *Pcdh15*$^{\Delta'CD2/\Delta'CD2}$ mutant mice, immunostainings for the three proteins are mostly located at the tips of the tall and middle-sized stereocilia and, to a lesser extent, of the persisting short stereocilia. Stereocilin and otogelin-like immunostainings can occasionally be seen extending between adjacent stereocilia towards the base of the hair bundle (arrows), whereas no such staining is observed for otogelin. (B) Scanning electron micrographs of the OHC hair bundles and TM in *Pcdh15*$^{+/\Delta'CD2}$ (a-c) and *Pcdh15*$^{\Delta'CD2/\Delta'CD2}$ mice (d-i) on P30 (b and e are higher magnifications of the areas boxed in a and d, respectively). In *Pcdh15*$^{\Delta'CD2/\Delta'CD2}$ mice, many stereocilia of the short row are missing (d). However, some OHC hair bundles may also have additional rows of stereocilia (see (g), where dots of five different colors identify five partial or complete rows of stereocilia). In keeping with the patterns of strong immunostainings for stereocilin, otogelin, and otogelin-like at the tips of middle-sized and short stereocilia (A), an overabundance of lateral links can be observed at this position, both within and between rows (dashed lines in e, h, and i). In many OHCs, some of the stereocilia of the middle row are of the same height as those of the short (yellow stars in h and i) or tall (red stars in h and i) rows, especially when the adjacent stereocilium in the tall row is missing (arrows in h). This observation may be directly linked to the abundance of inter-row links in an abnormal position at the tips of stereocilia (rather than subapical), suggesting that either horizontal top connectors (in their correct position) or PCDH15-CD2-containing links are required to establish or maintain the staircase pattern of the OHC hair bundles. Hair bundle imprints in the TM, with, locally, two rows of stereociliary imprints instead of one (stars in f), and embedded stereocilium tips (arrow in f) can be observed in *Pcdh15*$^{\Delta'CD2/\Delta'CD2}$ mice. Scale bars: 5 µm (fluorescence microscopy in A), 0.5 µm (scanning electron microscopy in A and panels b, e, h, i in B), 1 µm (panels a, d, g in B), or 2 µm (panels c, f in B).

References

1. Birling MC, Dierich A, Jacquot S, Herault Y, & Pavlovic G (2012) Highly-efficient, fluorescent, locus directed cre and FlpO deleter mice on a pure C57BL/6N genetic background. *Genesis* 50(6):482-489.
2. Lallemand Y, Luria V, Haffner-Krausz R, & Lonai P (1998) Maternally expressed PGK-Cre transgene as a tool for early and uniform activation of the Cre site-specific recombinase. *Transgenic Res* 7(2):105-112.
3. Verpy E*, et al.* (2008) Stereocilin-deficient mice reveal the origin of cochlear waveform distortions. *Nature* 456(7219):255-258.
4. Simmler MC*, et al.* (2000) Targeted disruption of otog results in deafness and severe imbalance. *Nat Genet* 24(2):139-143.
5. Lefèvre G*, et al.* (2008) A core cochlear phenotype in USH1 mouse mutants implicates fibrous links of the hair bundle in its cohesion, orientation and differential growth. *Development* 135(8):1427-1437.
6. Etournay R*, et al.* (2010) Cochlear outer hair cells undergo an apical circumference remodeling constrained by the hair bundle shape. *Development* 137(8):1373-1383.
7. Pepermans E*, et al.* (2014) The CD2 isoform of protocadherin-15 is an essential component of the tip-link complex in mature auditory hair cells. *EMBO Mol Med* 6(7):984-992.
8. Caberlotto E, Michel V, Boutet de Monvel J, & Petit C (2011) Coupling of the mechanotransduction machinery and F-actin polymerization in the cochlear hair bundles. *Bioarchitecture* 1(4):169-174.
9. Legan PK*, et al.* (2000) A targeted deletion in alpha-tectorin reveals that the tectorial membrane is required for the gain and timing of cochlear feedback. *Neuron* 28(1):273-285.
10. Mburu P*, et al.* (1997) Mutation analysis of the mouse myosin VIIA deafness gene. *Genes Funct* 1(3):191-203.
11. Verpy E*, et al.* (2011) Stereocilin connects outer hair cell stereocilia to one another and to the tectorial membrane. *J Comp Neurol* 519(2):194-210.
12. Furness DN, Katori Y, Nirmal Kumar B, & Hackney CM (2008) The dimensions and structural attachments of tip links in mammalian cochlear hair cells and the effects of exposure to different levels of extracellular calcium. *Neuroscience* 154(1):10-21.